TRANSITORY AERODYNAMIC FLOW CONTROL OF A PITCHING/PLUNGING AIRFOIL

Yuehan Tan
Woodruff School of Mechanical Engineering
Georgia Institute of Technology
771 Ferst Dr NW, Atlanta, Georgia 30332 USA
ytan@gatech.edu

Thomas M. Crittenden
Woodruff School of Mechanical Engineering
Georgia Institute of Technology
771 Ferst Dr NW, Atlanta, Georgia 30332 USA
thomas.crittenden@me.gatech.edu

Ari Glezer
Woodruff School of Mechanical Engineering
Georgia Institute of Technology
771 Ferst Dr NW, Atlanta, Georgia 30332 USA
ari.gelzer@me.gatech.edu

ABSTRACT

Transitory control and regulation of trapped vorticity concentrations are exploited in wind tunnel experiments for control of the aerodynamic loads on an airfoil moving in time-periodic pitch and coupled pitch-plunge motions beyond the dynamic stall margin. The presence of the pitch-coupled plunge delays lift and moment stall during upstroke and flow reattachment during downstroke, and results in significant degradation of pitch stability. Flow control actuation is effected using a spanwise array of integrated miniature chemical (combustion based) high-impulse actuators that are triggered intermittently relative to the airfoil's motion. The effects of the actuation on the aerodynamic characteristics of the airfoil are assessed using time-dependent measurements of the lift force and pitching moment and particle image velocimetry that are acquired phased-locked to the motion of the airfoil. It is shown that properly-timed single actuation pulse having a characteristic time scale that is an order of magnitude shorter than the airfoil's convective time scale has sufficient control authority to alter the global aerodynamic performance throughout the motion cycle. While actuating during the upstroke primarily affects the formation, evolution and advection of the dynamic stall vortex, actuating during the downstroke hastens reattachment compared to the base flow. Staged actuation using superposition of multiple discrete actuation pulses during the pitch/plunge cycle leads to enhancement of cycle lift and pitch stability, and reduce the cycle hysteresis and peak pitching moment.

INTRODUCTION

Dynamic stall of a pitching airfoil as it moves beyond its static stall limit is characterized by the rapid formation, advection and shedding of a large-scale concentration of vorticity and is accompanied by a sharp increase in nose-down pitching moment (moment stall), followed by a sizable drop in lift (lift stall, e.g., McCroskey, 1981). The stall typically occurs on retreating rotorcraft blades (between mid-span and tip) and the rapid changes in aerodynamic loading, strong hysteresis, and unstable damping severely limit the rotorcraft's operational characteristics and pose significant challenges for design of faster and more agile rotorcrafts with higher lift capacity.

Considering the transitory characteristics of dynamic stall, staged pulsed actuation appears to be particularly effective for mitigating its adverse aerodynamic effects as was amply demonstrated in the earlier works of Woo et. al. (2008, 2013), and Tan et. al. (2016). Woo et. al. (2008) demonstrated that pulsed actuation can lead to a brief collapse of the separated flow domain over a stalled static airfoil which can be achieved using a single actuation pulse having a characteristic time scale of $0.05T_{conv}$, resulting in a momentary change in circulation. By exploiting the disparity in duration between the onset and relaxation of the actuation effects (the latter is about 5-10 times longer) Woo et. al. (2013) used successive actuation pulses (up to 50) at equally-spaced time intervals during the pitching cycle to build up the effects of single pulse actuation. This approach was also used by Matalanis et al. (2014) to improve the aerodynamic characteristics of a pitching VR-12 airfoil at Mach numbers up to 0.5. In a later investigation, Tan et. al. (2016) showed that only a few (less than 6) discrete actuation pulses placed judiciously during critical instances of the pitching cycle yield control authority that leads to significant improvement in the aerodynamic performance that is

comparable or even exceeds the effects of multiple pulse actuation used by Woo et. al. (2013).

The present investigation builds on these earlier works and focuses on optimization of the actuation and their control authority by careful timing and superposition of independent actuation during the upstroke and downstroke using as few as two pulses. The actuation is investigated during pitch and in the presence of pitch-plunge motions.

EXPERIMENTAL SETUP

The present experiments utilize a modular VR-12 airfoil model integrated with a spanwise array of COMPACT actuators. The model has a cord c = 381 mm, spans the full width of the test section (910 mm), and includes endplates at its spanwise edges shown in Figure 1(a). The model is suspended at its quarter chord on an electromechanical 2-DOF traverse that can provide individually-programmable time-dependent pitch and plunge motions. In the present investigations the model is driven in nearly time-harmonic pitch and coupled pitch-plunge motions. It is noted that the addition of plunge motion to the pitching airfoil changes its kinematic angle of attack by $\beta(t) = \tan^{-1}(-\frac{1}{U_0}\frac{dh(t)}{dt})$ where $h(t)$ is the vertical displacement of the center of rotation and U_0 is the free stream velocity (Lian et. al., 2008). The airfoil's aerodynamic performance is characterized using time-resolved measurements of the lift and pitching moment and the angular and vertical positions of the airfoil. Inertia effects associated with the rotational and translational motion of the airfoil are measured with embedded accelerometers and are subtracted from global force data to produce the aerodynamic loads. Typical C_L-α and C_M-α variations are averaged over 200 oscillation cycles of the model, and additional performance parameters are given by the cycle

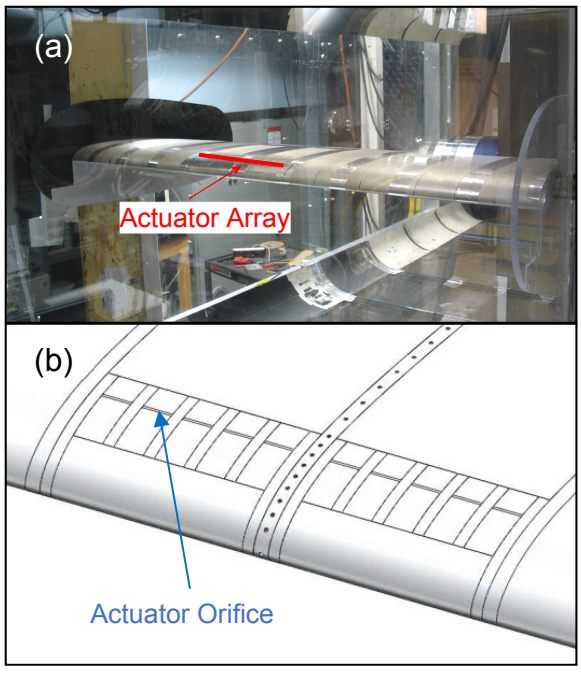

Figure 1. (a) The modular VR-12 airfoil model mounted in the wind tunnel, and (b) schematic of the actuation array.

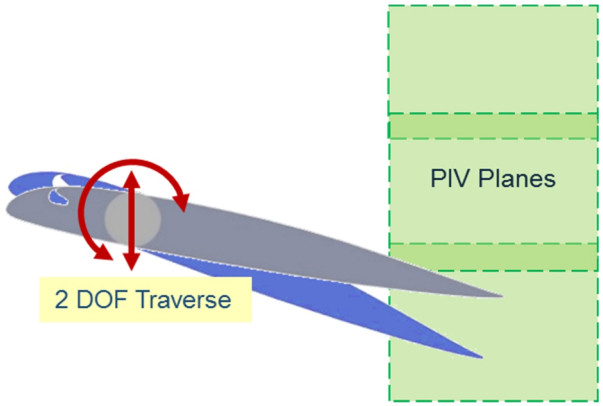

Figure 2. The airfoil 2-DOF motions along with the three partially overlapping PIV fields.

averaged lift, $\langle C_L \rangle = \frac{\int C_L dt}{T_{cycle}}$, hysteresis coefficient $H_\alpha = \oint C_L d\alpha$, and cycle damping coefficient $\Xi_\alpha = -\frac{\oint C_M d\alpha}{\pi \alpha_A^2}$ (Carta, 1967).

In the present investigations, the airfoil's pitch range (static stall occurs at α = 16°) is $10 \le \alpha \le 20$, at 2 Hz (reduced frequency $k = \pi f c/U_0 = 0.12$). In the pitch-plunge motion the peak-to-peak displacement is h = 0.05c, at 2 Hz (k = 0.12) with no phase difference between the two trajectories. The experiments are conducted at Re_c = 504,000.

The actuator arrays are arranged in two banks each comprising five COMPACT actuators that are arranged symmetrically about mid-span and occupy 21% of the model's span. Therefore, the incremental changes in aerodynamic loads that are associated with the actuation represent about a fifth of the increments that can be achieved with full-span actuation. The actuator banks are separated by a module of fifty-two static pressure taps as shown schematically in Figure 1(b). The actuators' orifices are located at x/c = 0.1, and each actuator has a rectangular orifice measuring 12.7 × 0.35 mm. Transitory flow control is achieved by intermittent actuation pulses that are triggered from the laboratory computer so that the actuation timing is phase-locked to the airfoil's motion.

The flow in cross stream (x-y) plane over the suction surface near the model's trailing edge and in its near wake is measured phase-locked to the pitch motion of the airfoil using particle image velocimetry (PIV) to demonstrate the effects of the actuation during upstroke and downstroke motions. Three PIV camera positions are used, and the phase-averaged flow fields are subsequently stitched together to form a single domain measuring 0.5c × 0.9c as shown in Figure 2.

RESULTS AND DISCUSSION

Base Flow Characteristics

The variations of the phase-averaged lift C_L-α and pitching moment C_M-α during pitch (P) and pitch-plunge (P-P) motions of the airfoil along with the corresponding trajectories of effective angle of attack and tail excursion velocity are shown in Figures 3(a-d), respectively. Note that the addition of the plunge motion results in slight decrease and increase in total angle of attack during upstroke and downstroke motions, respectively. More importantly,

the magnitude of the trailing edge velocity in the presence of plunge decreases significantly throughout the cycle (up to 43% in the mid-point of up- and downstroke motions).

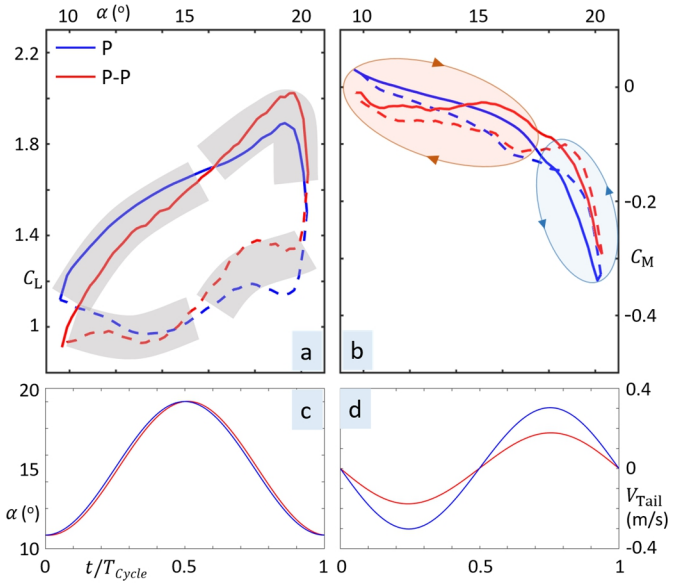

Figure 3. Phase averaged C_L-α (a) and C_M-α (b) for base airfoil in nearly time harmonic **pitch** and **pitch-plunge** motions. The upstroke and downstroke segments are marked with solid and dashed lines, respectively. Also shown are the variations of the effective AoA (c) and tail excursion speed (d) during the cycle.

It is instructive to compare C_L-α and C_M-α within the different regimes of the *P* and *P-P* cycles. While during the upstroke ($10^o\uparrow < \alpha < 15^o\uparrow$) the lift of *P* and *P-P* increases nearly linearly with α, $\dot{\alpha}$ is lower for *P-P* [Figure 3(c)], especially at low α. As noted by Tupper (1983) $dC_L/d\alpha$ for thin airfoils is inversely related to $\dot{\alpha}$, and therefore $dC_L/d\alpha$ is lower for *P-P* in this domain. On the other hand, changes in C_M-α are mostly governed the growth of a local separation bubble upstream of the trailing edge, which can be sensitive to the tail velocity. The significantly reduced tail velocity in *P-P* restricts the growth and upstream travel of this separation bubble, which explains why pitching moment in *P-P* remains nearly invariant until the formation of the dynamic stall vortex at $\alpha > 16^o$. However, the restricted growth of the separation bubble also results in an overall lower *P-P* lift in this domain.

The formation, advection, and shedding of the dynamic stall vortex cycle occurs within the domain $16^o\uparrow < \alpha < 19^o\downarrow$. The vortex originates near the leading edge and contributes significantly to the accumulation of CW vorticity and increase in lift as it is advected downstream. The shift in loading distribution results in rapid decrease in pitching moment. It appears that the reduced relative surface velocity in *P-P* (as the airfoil is moving away from the flow at a slower rate) enhances the strength of the vortex while delaying its shedding (by 0.7° compared to *P*) and thereby and leads to higher lift. While the shedding of vortex in *P-P* is more abrupt, these data suggest that less vorticity is shed since the decrease in lift during stall is 10% lower than in *P*.

Table 1. Global aerodynamic performance for base airfoil

Motion	$\langle C_L \rangle$	C_{L-max}	H_α	C_{M-max}	Ξ_α
Pitch	1.35	1.89	0.10	-0.34	-0.07
Pitch-Plunge	1.35	2.02	0.09	-0.29	-0.15

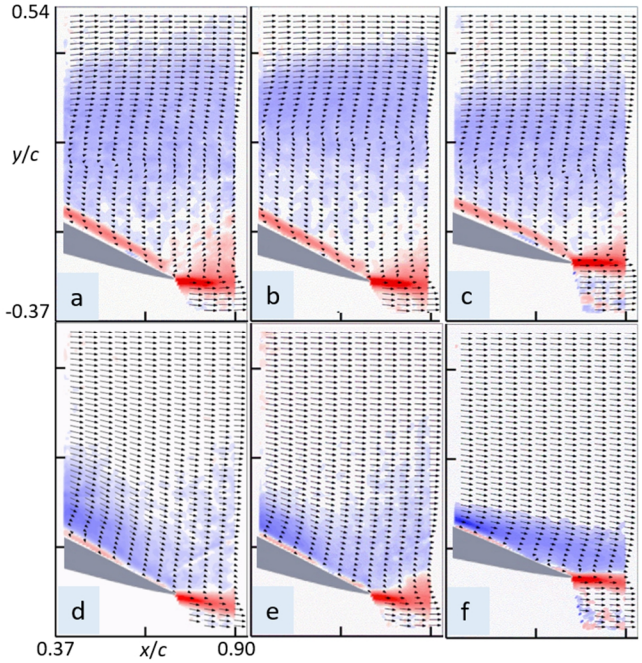

Figure 4. Color raster plots of spanwise vorticity superposed with velocity vectors upstream of the trailing edge and in the near wake for the base flow (a-c) and in the presence of actuation (d-f): $\alpha = 18.75^o\uparrow$ (a, d), $18.5^o\downarrow$ (b, e), and $14^o\downarrow$ (c, f).

The airfoil is completely stalled as it begins its downstroke motion ($16^o\downarrow < \alpha < 19^o\downarrow$) where the lift decreases from a level that is considerably lower than pre-stall at the upstroke (C_L at *P-P* is higher than *P*). Despite the decrease in α, C_M rapidly increases as following the shedding of the stall, where the rate of increase is higher for *P-P*. However, because the plunge motion of the airfoil (towards the free stream) and the larger effective α, during *P-P* the reattachment is slower and rate of decrease $dC_L/d\alpha$ is higher than during *P*, leading to diminution of the positive damping for the C_M loop of *P-P* between 16° and 20°. As the downstroke continues ($10^o\downarrow < \alpha < 16^o\downarrow$) the flow begins to reattach and the C_L increases for *P* and decreases at a slower rate for *P-P*. The slowed reattachment because of the plunge motion (the aft segment of the chord is moving towards the free stream at a slower rate than in pitch only) the recovery of the pitching moment is slower and consequently the negative damping intensifies compared to the *P* cycle.

Table 1 lists the various global parameters for the *P* and *P-P* cycles of the base airfoil including the cycle-averaged lift $\langle C_L \rangle$, maximum lift C_{L-max}, hysteresis coefficient H_α maximum moment C_{M-max}, and the damping coefficient Ξ_α.

Pulsed Actuation on a Pitching Airfoil

As shown by Woo et. al. (2008), single actuation pulse during the upstroke of a pitching 2D airfoil can effectively sever the separated vorticity layer, trigger the collapse of the separated domain and the shedding of a large-scale concentration of CCW vorticity, and lead to transitory flow attachment followed by renewed separation. Pulsed actuation exploits the disparity between the characteristic times of the actuation onset O(1-2T_{conv}) and relaxation O(10-15T_{conv}) and induces significant changes in the aerodynamic performance throughout the entire time-periodic pitch cycle. Woo et al. (2013) used multiple actuation pulses during the pitch cycle to enhance the effects of the actuation on the aerodynamic performance and increase lift and pitch stability.

In follow-on investigations Tan et.al. (2016) explored the effects of superposition of discrete actuation pulses on the aerodynamic performance of a pitching airfoil ($k = 0.06$, $10 \le \alpha \le 20$) and showed that *when the actuation is applied on only 21% of the airfoil's span* staging of the actuation pulses during key instances of the motion cycle can lead up to 5.6% increase in cycle-averaged lift and up to three times increase in pitch stability. Remarkably, these improvements in performance can be achieved with as few as three actuation pulses during the pitch cycle. The effects of the actuation on the flow field upstream of the trailing edge of the airfoil and in its near wake were later measured using PIV. Figure 4 shows color raster plots of spanwise concentrations of vorticity superposed with velocity vectors in the absence (a-c) and presence (d-f) of actuation at $\alpha = 18.75^{o}\uparrow$ (a, d), $18.5^{o}\downarrow$ (b, e), and $14^{o}\downarrow$ (c, f). In the absence of actuation, these data capture stages in the shedding of the dynamic stall vortex immediately before and after the end of the upstroke segment of the motion [Figures 4(a) and (b)] showing that the nominal cross stream width of the vortex is 0.65c. While width of the separated flow domain diminishes during the downstroke, the flow is clearly not yet fully reattached at $\alpha = 14^{o}\downarrow$. When a single actuation is applied at nominally $t/T_{cycle} = 0.35$ ($\alpha = 18^{o}\uparrow$), the actuation apparently leads to partial rollup and some shedding of the CW surface vorticity (as seen on the right-hand side of the Figures 4(d)(e) ($x/c > 0.68$) that is followed by a relatively thin vorticity layer and a closed recirculation bubble near the surface as is evidenced by the isolated domain of CCW vorticity upstream of the trailing edge. This closed vorticity domain is the precursor to full separation that follows as the downstroke proceeds, but is significantly slower than the separation in the absence of actuation. It is also noted that the application of an additional single actuation pulse at $t/T_{cycle} = 0.71$ ($\alpha = 16^{o}\downarrow$), leads to nearly full attachment indicating the capability to restore some of the lift and reduce the cycle hysteresis.

Staged Actuation: Pitch and Pitch-Plunge Motions

The measurements in Figure 4 help identify two critical stages during the pitch cycle where the flow would be most receptive to pulsed actuation, namely, just before moment stall during the upstroke, and during the downstroke when the reattachment appears to be delayed until nearly the change in motion direction to upstroke. Actuation during the upstroke ahead of the moment stall can alter the formation and evolution of the dynamic stall vortex and result in strong changes in the rate of vorticity flux into the near wake that clearly affects the magnitude of circulation and

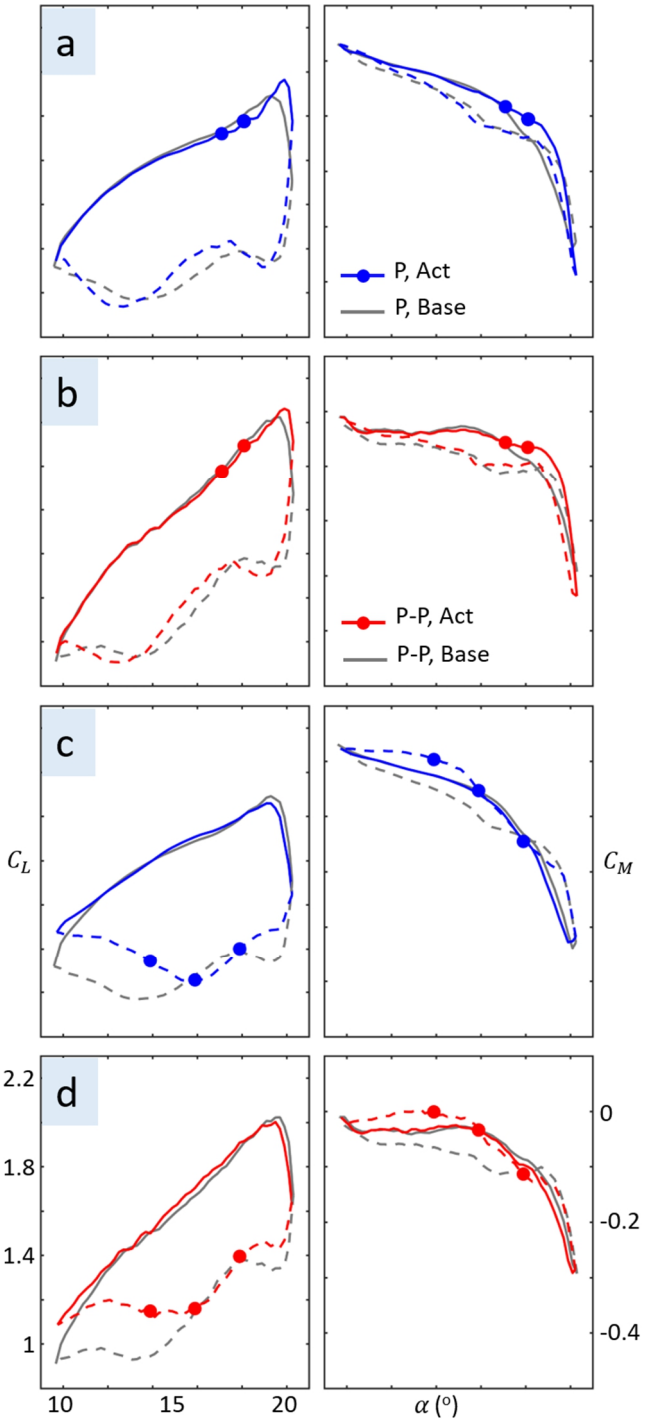

Figure 5. Phase plots of C_L-α (left column) and C_M-α (right column) for actuation during **pitch** and **pitch-plunge** motions: upstroke (a, b) and downstroke (c, d). The upstroke and downstroke motions are marked using solid and dashed lines, respectively. Each dot indicates a single actuation pulse.

lift following the stall during the downstroke. Actuation during the downstroke can accelerate flow reattachment, reduce the cycle hysteresis and potentially improved pitch stability. Following the

discussion in connection with Figure 3, the aerodynamic performance enhancement associated with actuation programs that focus on these stages are characterized during pitch and coupled pitch-plunge motions and are described in Figure 5. The timing of the actuation which is optimized for the pitch motion is also used in the presence of the plunge.

The first actuation program (*P-US*) is intended to maintain or extend flow attachment near the leading edge and regulate the progression growth of trailing edge separation bubble and evolution of dynamic stall vortex. The application of two discrete actuation pulses at 17° ↑ (t/T_{cycle} = 0.32) and 18° ↑ (t/T_{cycle} = 0.35) during the pitch cycle [Figure 5(a)] slows the growth of the vortex as is evidenced by the increase in $C_{L\text{-}max}$ (by 8.5%) through 20.5°↑ (up from 19°↑ in base flow). The actuation also leads to higher level of C_M than in the base flow that also increases the negative damping which decrease the overall damping coefficient significantly (from -0.07 to -0.18). This actuation program has similar effects in the presence of pitch-plunge [Figure 5(b)], although the improvement over the base flow is somewhat lower. It is noted, however, that in the presence of pitch-plunge the corresponding decrease in the damping coefficient compared to the pitch motion is noticeably lower (-0.05 vs -0.11) because of the lower downward speed of the trailing edge. It is also noteworthy that the increase in lift following the actuation affects the motion following stall during the downstroke indicating that the change in vorticity flux affects the circulation until the upstroke commences again.

Pulsed actuation during the downstroke [*P* and *P-P,* Figures 5(c) and (d), respectively] is applied using a sequence of three consecutive pulses (*P-DS*) at α = 18°↓, 16°↓, and 14°↓ (t/T_{cycle} = 0.65, 0.72, and 0.78, respectively) that commences when the flow is fully separated. The actuation accelerates the reattachment process throughout downstroke resulting in a significant increase in lift and pitch stability. To begin with, the actuation suppresses the momentary reduction in lift following the shedding of the dynamic tall vortex (that peaks at $\alpha \approx$ 19°↓in the absence of actuation). This is remarkable because the actuation is applied following this diminution, and indicates that there is a global regulation in the shedding of vorticity into the wake during the motion cycle. The actuation also leads to a strong increase in C_L through the end of the downstroke that is accompanied by reduction in cycle hysteresis (cf. Table 2), and this increase appears to permeate even into the beginning of the following upstroke. The effects actuation appears to be somewhat more pronounced during pitch-plunge, ostensibly as a result of the slower reattachment process during this stage. The effects of the actuation on the pitching moment are also quite pronounced. In these segments of the cycle negative damping is nearly eliminated by the shift in the aerodynamic loadings towards the leading edge, resulting in a strong increase in pitch stability (cf. table 2).

The effects of (sequential) superposition of the upstroke and downstroke actuation programs were also tested for *P* and *P-P* motions and the effects on the lift and pitching moment are shown in Figures 6(a) and (b), respectively (the global aerodynamic parameters are included in Table 2). These data demonstrate that *the effects of the separate actuation programs are nearly additive and virtually independent, indicating little nonlinear effects that may arise from unsteady aerodynamics.* As shown in Figure 6, the stall delay and peak lift improvement effected by *P-US* are still observed with the addition of *P-DS*, while the lift and moment recovery during downstroke under *P-DS* is nearly unaffected by the addition of *P-US*. However, it is worth noting that such superposition should take into account certain conflicting or opposite effects of the actuation programs. For example, *P-US* increased C_M during upstroke, which in turn increases the negative damping, whereas *P-DS* promotes positive damping. While the resultant effect lies between these two programs, there is still significant improvement over the base flow. Finally, it is noted that the aerodynamic performance in the presence of actuation during pitch-plunge is very comparable to the effects during pitch only indicating that plunge motion does not hinder the performance of superposed actuation.

Table 2. Global aerodynamic performance under actuation*

Program	$\langle \Delta C_L \rangle$		ΔC_{L-max}		ΔH_α		$\Delta \Xi_\alpha$***	
	P	P-P	P	P-P	P	P-P	P	P-P
Base flow**	1.35	1.35	1.89	2.05	0.10	0.09	-0.07	-0.15
P-*US*	1.1%	1.1%	8.5%	4.2%	-5.6%	-5.4%	-0.11	-0.05
P-*DS*	4.1%	5.2%	-0.2%	-0.1%	-19.7%	-21.4%	0.23	0.26
P-*US*+P-*DS*	4.3%	4.5%	6.3%	3.9%	-16.2%	-15.6%	0.05	0.09

* Only 21% actuated span. ** Actual value *** $\Delta \Xi_\alpha$ incremental value relative to the (low) base damping

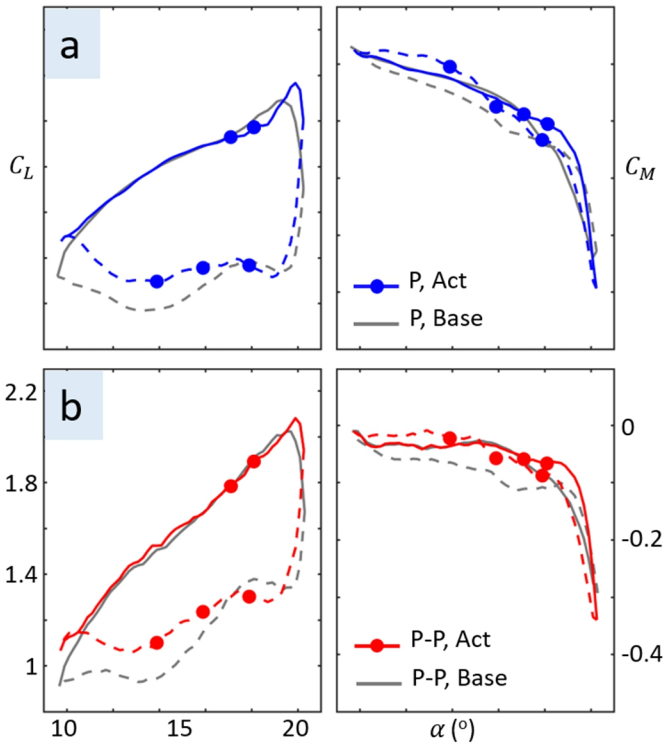

Figure 6. Superposition of *P-US* and *P-DS* in pitch (a) and pitch-plunge (b) motions.

CONCLUSION

The effectiveness of a transitory pulsed actuation for controlling the aerodynamic loads on an airfoil moving in time-periodic pitch and coupled pitch-plunge motions beyond the dynamic stall margin is investigated in wind tunnel experiment. It is shown that the presence of pitch-coupled plunge delays lift and moment stall during upstroke and flow reattachment during downstroke, and results in significant degradation of pitch stability. Pulsed actuation is realized using an array of chemical (combustion) powered actuators single having a characteristic time scale of $0.05T_{conv}$, that that are triggered intermittently relative to the airfoil's motion. By exploiting the disparity in duration between the onset and relaxation of the actuation effects (the latter is about 5-10 times longer) successive actuation pulses can build up the actuation effects. The effects of the actuation on the aerodynamic characteristics of the airfoil are assessed using a range of actuation timing that lead to varies degrees of improvements in lift, pitch stability and hysteresis. The present investigation emphasizes the global control effectiveness of separate actuation sequences comprising few discrete actuation pulses during two critical stages in the upstroke and downstroke segments. While upstroke actuation regulates the formation and growth of the dynamic stall vortex resulting in delayed stall and improved lift, downstroke actuation accelerates flow reattachment improves the pitch stability and reduces hysteresis. The actuation effectiveness is more pronounced during the downstroke when the base flow is fully separated. The present investigations demonstrate that the effects of the separate actuation programs are nearly additive and virtually independent. However, superposition of separate programs should take into account individual conflicting or opposite effects (e.g., different trends in pitch stability). Although the presence of the plunge motion alters the performance of the pitch cycle significantly, it does not render the actuation less effective. In most the cases, plunge motion is enhances the receptivity of the flow to actuation and the aerodynamic performance may be may be further improved by further tuning of the actuation timing.

ACKNOWLEDGEMENT

This work is supported by Georgia Tech VLRCOE and UTRC/NASA.

REFERENCES

Brzozowski, D., Woo, G., Culp, J., Glezer, A. 2010, "Transient Separation Control using Pulse-Combustion Actuation", *AIAA J.*, **48**, 2482-2490.

Carta, F.O., 1967, "An analysis of the stall flutter instability of helicopter rotor blades", *Journal of the American Helicopter Society*, 12(4), pp.1-18.

Crittenden, T., Warta, B., and Glezer, A., 2006, "Characterization of Combustion Powered Actuators for Flow Control", *AIAA Paper 2006-2864*, 3rd AIAA Flow Control Conference, San Francisco, CA.

Lian, Y., Ol, M. and Shyy, W., 2008, "Comparative study of pitch-plunge airfoil aerodynamics at transitional reynolds number", *46th AIAA Aerospace Sciences Meeting and Exhibit* (p. 652).

Matalanis, C., Min, B.-Y., Bowles, P., Jee, S., Wake, B., Crittenden, T., Woo, G., and Glezer, A., 2014, "Combustion-Powered Actuation for Dynamic Stall Suppression – Simulations and Low-Mach Experiments", *Annual Forum Proceedings - AHS International*, v 3, p 1817-1830.

McCroskey, W.J., 1981, "*The phenomenon of dynamic stall*", (No. NASA-A-8464). NASA, Moffett Field, CA

Tupper, K.W., 1983, "The Effect of Trailing Vortices on the Production of Lift on an Airfoil Undergoing a Constant Rate of Change of Angle of Attack", *Thesis*, Air Force Institute of Technology, Wright-Patterson AFB, OH.

Woo, G., Crittenden, T., and Glezer, A., 2008, "Transitory Control of a Pitching Airfoil Using Pulse Combustion Actuation", *AIAA Paper 2008-4324*, 4th AIAA Flow Control Conference, Seattle, WA.

Woo, T. K. and Glezer, A., 2013, "Controlled transitory stall on a pitching airfoil using pulsed actuation", *Exp Fluids*, **54**, 1507.